JOURNAL OF
Materials
CHEMISTRY

Synthesis, structural chemistry and magnetic properties of $La_{1+x}A_{1-x}InMnO_{6-\delta}$: A = Ba, Sr; $x = 0, 0.2$

Peter D. Battle,[*a] **Amalia I. Coldea,**[b] **Nicola A. Jordan,**[a] **Matthew J. Rosseinsky**[*a]† **and John Singleton**[b]

[a]*Inorganic Chemistry Laboratory, University of Oxford, South Parks Road, Oxford, UK OX1 3QR*
[b]*Clarendon Laboratory, Department of Physics, University of Oxford, Parks Road, Oxford, UK OX1 3PU*

Received 24th January 2001, Accepted 9th April 2001
First published as an Advance Article on the web 2nd May 2001

A series of novel double perovskites $La_{1+x}A_{1-x}InMnO_{6-\delta}$ (A = Sr, Ba) has been prepared and the room temperature crystal structures have been refined using X-ray and neutron powder diffraction. In all cases the B-site is occupied by a disordered arrangement of In^{3+} and $Mn^{3+/4+}$ cations. However, whereas $La_{1+x}Ba_{1-x}InMnO_{6-\delta}$ exhibits two octahedral tilts and exists in a body-centred cell, space group *Imma*, $La_{1+x}Sr_{1-x}InMnO_{6-\delta}$ adopts the three-tilt $GdFeO_3$ structure and has a primitive orthorhombic structure, space group *Pnma*. Magnetic susceptibility data show that all the compositions synthesised exhibit a spin glass freezing transition at ~8 K. A negative magnetoresistance $\Delta\rho/\rho_0 = 10.5\%$ was measured at 164 K in a field of 14 T.

Introduction

Complex, mixed-valence oxides of manganese with a perovskite-type structure, for example $La_{1-x}Sr_xMnO_3$, have been shown to exhibit a wide variety of interesting structural and physical properties, including charge ordering, magnetic ordering and colossal magnetoresistance (CMR). This has led to a great deal of interest in their behaviour and, in the search for enhanced CMR properties, some recent attention has centred upon the consequences of doping the manganese site.[1,2] It has been shown that in charge-ordered Mn^{3+}/Mn^{4+} regimes, doping with as little as 3% of a tri- or tetravalent cation can destroy the charge-ordering and induce CMR properties,[3] and a recent investigation of $CaMn_{1-x}M_xO_3$ (M = Nb, Ta, W, Mo) has shown that CMR properties can also be induced by doping the B site with higher valency cations. This strategy introduces mixed-valence manganese and consequently the possibility of double exchange.[4] Our own work[5–7] has shown that doping Mn perovskites and K_2NiF_4 phases with diamagnetic Rh^{3+} can induce ferromagnetic behaviour in insulating $Mn^{3+/4+}$ oxides, with a magnetoresistance maximum being observed at the Curie temperature in the case of $La_{1.5}Sr_{0.5}MnRhO_6$.

In the study described below, a series of double perovskites with a 1 : 1 ratio of indium to manganese on the B-cation site was synthesised. This stoichiometry can be accommodated with a disordered arrangement of cations on the B sub-lattice or with one of two ordered cation arrangements, these being layered or rocksalt-like in nature (Fig. 1). Previous studies have suggested that many factors, including the size, charge and co-ordination preference of the cations, all have a role to play in determining which arrangement is adopted.[8] In particular, the layered structure is associated with the presence of a d^{10} cation, and we were keen to determine whether the introduction of In^{3+} would enable us to prepare perovskites containing layers of MnO_6 octahedra separated from each other by layers of InO_6 octahedra. In addition to modifying the structural chemistry, diluting the manganese sub-lattice with a fixed valence, diamagnetic post-transition metal will modify the magnetic behaviour of the material in a manner which depends upon the extent and nature of any cation ordering. Despite the absence of any such long-range ordering, doping 50% Ga^{3+} onto the B-site of $LaMnO_3$ and $NdMnO_3$ has been shown to alter strongly the magnetic behaviour whilst preserving the manganese oxidation state at +3.[9] The extent of the static coherent Jahn–Teller distortion associated with Mn^{3+} controls the magnetism in these phases. This paper complements that study by describing an investigation of $LaBaInMnO_{6-\delta}$ in which the d^{10} cation In^{3+} is used to dilute an array of Mn cations with a mean oxidation state close to +4. Other compositions $La_{1+x}A_{1-x}InMnO_{6-\delta}$ (A = Ba, Sr), prepared in an attempt to lower the mean oxidation state, are discussed briefly.

Experimental

Polycrystalline samples, which will be referred to initially by their nominal composition $La_{1+x}A_{1-x}InMnO_6$; A = Ba or Sr, were synthesised using standard ceramic techniques. Stoichiometric quantities of high purity (Alfa Puratronic® or Aldrich; minimum purity 99.994%) $BaCO_3$, $SrCO_3$, La_2O_3 (dried), In_2O_3 and MnO_2 were intimately mixed in an agate mortar and pestle and heated in air at 800 °C for 1 day as a loose powder, and then as pellets at 1000 °C and 1200 °C. Finally the mixture was heated for one day at each of 1250, 1300, 1350, 1400 and 1450 °C. Regrinding was undertaken daily to ensure sample homogeneity. The progress of the reaction was monitored by X-ray powder diffraction (XRD) and data were collected on the final products using a Siemens D5000 diffractometer operating in Bragg–Brentano geometry with Cu $K_{\alpha 1}$ radiation. Data were collected over the angular range $15 \leqslant 2\theta/° \leqslant 120$ with a step size of $\Delta 2\theta = 0.02°$. Neutron diffraction data were collected on a 2.7 g sample of $LaBaInMnO_6$ at room temperature and 5 K on the D2b instrument at the ILL in Grenoble, France. The sample was mounted in a cylindrical, 5 mm diameter vanadium can and the diffraction pattern was collected over the *d*-spacing range $0.835 < d/Å < 6.133$ using radiation with $\lambda = 1.594$ Å. An ILL 'orange' cryostat was used

---

†Present address: Department of Chemistry, University of Liverpool, Liverpool, UK L69 7ZD.

DOI: 10.1039/b100840o

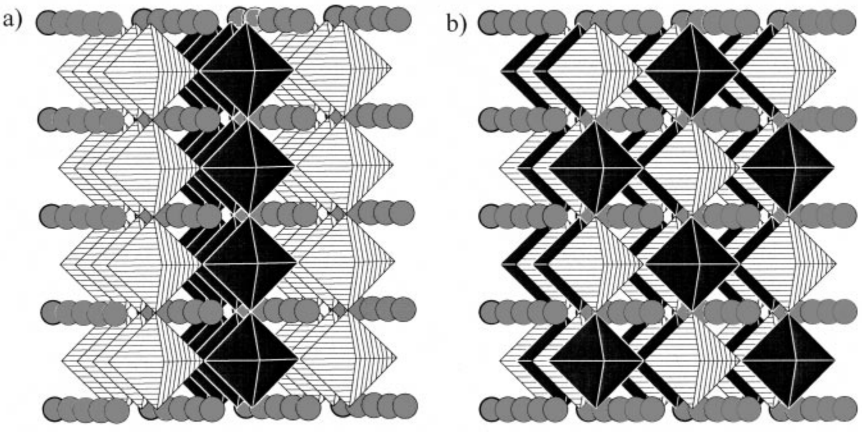

Fig. 1 Ordered arrangements of cations in $A_2BB'O_6$ perovskites: a) layered; b) rocksalt-type.

for the measurement taken at 5 K. Analysis of the X-ray and neutron data was carried out by the Rietveld method[10] using the GSAS suite of programs,[11] the neutron diffraction data having been previously corrected for absorption. The temperature factors of the oxygen atoms were fixed at constant values in the refinements where only X-ray data were considered; this prevented them from refining to physically meaningless values. Electron diffraction patterns were obtained for $LaBaInMnO_6$ using a JEOL 2000FX electron microscope equipped with a double-tilt specimen holder. Finely ground samples were dispersed in hexane and mounted on to lacey carbon-coated copper grids (300 mesh). Magnetic susceptibility measurements were made using a Quantum Design MPMS-5 SQUID magnetometer. Data were collected after cooling the sample to 5 K both in the absence (ZFC) and presence (FC) of the measuring field of 100 Oe. Magnetoresistance measurements were carried out on a sintered bar of the composition $La_{1.2}Ba_{0.8}InMnO_6$ using the standard four-terminal method with a direct current of less than 10 μA. The magnetic field was applied perpendicular to the current direction.

Results

a) Structural chemistry

Monophasic polycrystalline samples of $La_{1+x}A_{1-x}InMnO_6$ were successfully synthesised for $x=0$, 0.2 for A = Ba and $x=0.2$ for A = Sr. Attempts to prepare other compositions ($x=0.4$, 0.6, 0.8 A = Ba and $x=0$, 0.4, 0.6, 0.8 A = Sr) by the method described above were unsuccessful. However, it is worth noting that the multiphasic nature of some of these compositions was only recognised during screening by neutron diffraction, the sample having appeared monophasic when examined by XRD. The X-ray diffraction patterns collected for each of the monophasic samples were indexed using a unit cell of dimensions $\sim\sqrt{2}a_p \times \sim 2a_p \times \sim\sqrt{2}a_p$, where a_p is the lattice constant of the simple ABO_3 cubic perovskite. Sample insolubility prevented the determination of oxygen content by volumetric analysis.

For $La_{1+x}Ba_{1-x}InMnO_6$ $x=0$, 0.2 a body-centred cell was used to index all the observed reflections in the XRD data. The absence of any visible reflections below $2\theta=20°$ in the X-ray diffraction pattern suggested that the B-site cations are disordered. Only four tilt systems,[12] corresponding to the space groups *I*4/*mcm* (tetragonal), *Imma* (orthorhombic), *I*2/*b* (monoclinic) and *I*2/*m* (monoclinic), are compatible with such a cell. The electron diffraction data collected for the $x=0$ (Fig. 2) sample rule out the tetragonal space group *I*4/*mcm*, the condition for *h*0*l* reflections (*h*, $l=2n$) being violated. Unfortunately these data cannot be used further to distinguish between the orthorhombic and monoclinic space groups. However, analysis of the room temperature X-ray and neutron diffraction data (Fig. 3) clearly showed the space group of $LaBaInMnO_6$ to be *Imma*; refinement of this model proceeded smoothly, whereas the refinements attempted using the

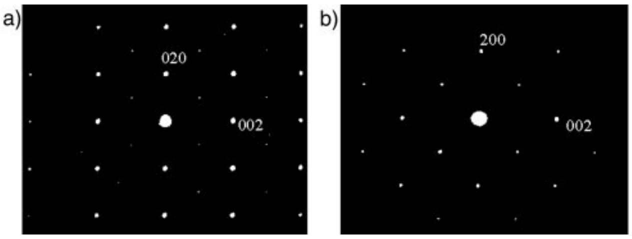

Fig. 2 Electron diffraction data for a) [100] and b) [010] zone axes of $LaBaInMnO_6$.

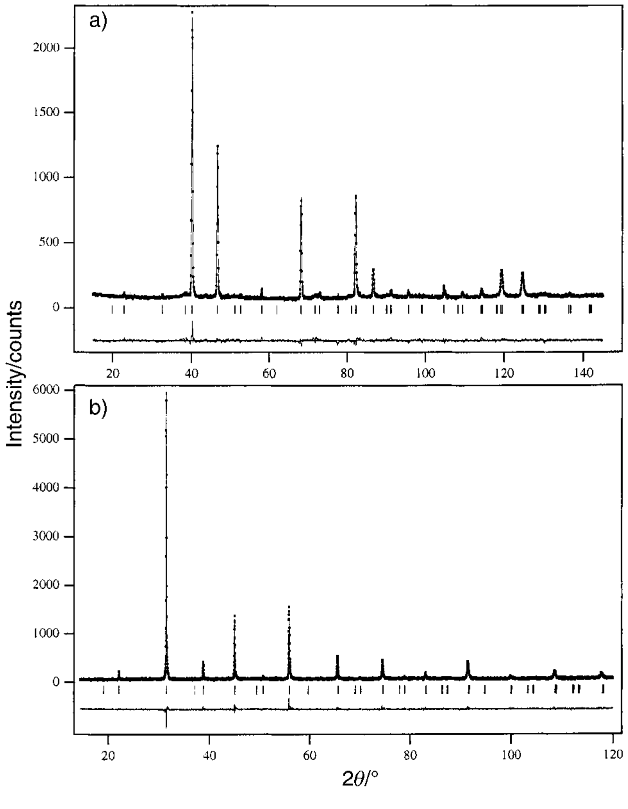

Fig. 3 Observed (dots), calculated (line) and difference profiles from Rietveld refinement of $LaBaInMnO_6$ at 300 K: a) neutron and b) X-ray data. Reflection positions are indicated.

Table 1 Structural parameters for $LaBaInMnO_{6-\delta}$ at room temperature

Space group: *Imma*

	R_{wp}	R_p	χ^2
X-ray histogram	0.1144	0.0907	—
Neutron histogram	0.0688	0.0517	—
Powder total	0.0869	0.0774	1.437

$a=5.6944(3)$, $b=8.0548(4)$, $c=5.6826(3)$ Å, $V=260.65(3)$ Å^3

	Site	x	y	z	U_{iso}/Å^2
La/Ba	4e	0	0.25	−0.002(2)	0.0141(4)
In/Mn	4b	0	0	0.5	0.0001(8)
O1	4e	0	0.25	0.482(2)	0.039(3)
O2	8g	0.25	0.012(1)	0.75	0.053(2)

monoclinic space groups were unstable. The electron diffraction data, indexed in space group *Imma*, are shown in Fig. 2. These data demonstrate the absence of structural complexity (for example, cation ordering) over distances shorter than those sampled by neutron or X-ray diffraction.

The neutron diffraction data confirmed the absence of ordering among the B-site cations. Ordering would have been immediately apparent in these data given the substantial difference in scattering length between In and Mn (0.406 fm and −0.373 fm respectively).[13] It was in fact necessary to refine the room temperature neutron and X-ray diffraction data simultaneously because of the negligible overall neutron scattering from the B-site. The refined structural parameters of $LaBaInMnO_6$ are shown in Table 1. The occupation factors of the O1 and O2 sites did not decrease in trial refinements and they were consequently held fixed at a value of unity in the final refinements. Selected bond distances and angles are shown in Table 2 and it can be seen that the mean In/Mn–O bond distance is in good agreement with that predicted from published tables of ionic radii (2.015 Å).[14] The XRD data for the $x=0.2$ sample were also analysed successfully in this space group (Table 3).

In contrast to those data collected on the Ba-containing samples, the XRD data collected for $La_{1.2}Sr_{0.8}InMnO_6$ showed evidence for the adoption of a primitive unit cell. They were analysed in the space group *Pnma*, corresponding to the $GdFeO_3$ structure (Fig. 4, Table 4).

Table 2 Selected interatomic distances (Å) and bond angles (°) for $LaBaInMnO_{6-\delta}$ at room temperature

Mn/In–O1 × 2	2.0160(5)
Mn/In–O2 × 4	2.0135(4)
Mn/In–O1–Mn/In	174.5(6)
Mn/In–O2–Mn/In	174.5(5)

Table 3 Structural parameters for $La_{1.2}Ba_{0.8}InMnO_{6-\delta}$ at room temperature

Space group: *Imma*

	R_{wp}	R_p	χ^2
X-ray histogram	0.1146	0.0895	1.319

$a=5.6686(2)$, $b=8.0397(4)$, $c=5.6860(3)$ Å, $V=259.13(2)$ Å^3

	Site	x	y	z	U_{iso}/Å^2
La/Ba	4e	0	0.25	0.001(1)	0.0096(6)
In/Mn	4b	0	0	0.5	0.0075(8)
O1	4e	0	0.25	0.56(1)	0.005
O2	8g	0.25	0.042(4)	0.75	0.005

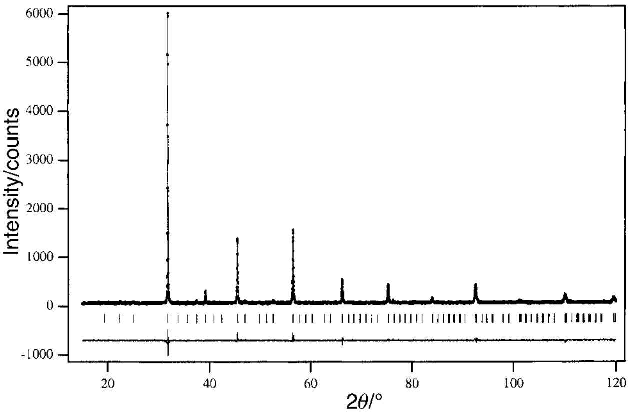

Fig. 4 Observed (dots) calculated (line) and difference profiles from Rietveld refinement of $La_{1.2}Sr_{0.8}InMnO_6$ at 300 K—space group *Pnma*. Reflection positions are marked.

Table 4 Structural parameters for $La_{1.2}Sr_{0.8}InMnO_{6-\delta}$ at room temperature

Space group: *Pnma*

	R_{wp}	R_p	χ^2
X-ray histogram	0.1110	0.0867	1.179

$a=5.6387(2)$, $b=7.9664(3)$, $c=5.6460(2)$ Å, $V=253.62(1)$ Å^3

	Site	x	y	z	U_{iso}/Å^2
La/Sr	4c	−0.0203(5)	0.25	−0.002(2)	0.0084(9)
In/Mn	4b	0	0	0.5	0.004(1)
O1	4c	0.502(4)	0.25	0.062(6)	0.005
O2	8d	0.225(6)	0.044(3)	0.787(5)	0.005

b) Magnetic behaviour

Analysis of the neutron diffraction data collected on $LaBaInMnO_6$ at 5 K proceeded smoothly within a model which considered only nuclear scattering and converged to reliability factors of $R_{wp}=6.97$, $\chi^2=1.389$. No significant changes in either the bond lengths or the bond angles were observed on cooling from room temperature. This analysis confirmed the absence of long range magnetic ordering. For each of the samples, a single magnetic transition takes place at a low temperature (typically $T_g \sim 8$ K) with a marked difference between zero field cooled (ZFC) and field cooled (FC) susceptibilities below this temperature; a smaller difference persists to higher temperatures. The data for $LaBaInMnO_6$ and $La_{1.2}Ba_{0.8}InMnO_6$ are shown in Fig. 5, and very similar data were obtained for $La_{1.2}Sr_{0.8}InMnO_6$. The magnetisation of $LaBaInMnO_6$ as a function of applied field at 5 K and 25 K is shown in Fig. 6. A hysteresis loop of finite width, symmetrical about the origin, was observed in each case, although at 300 K, the magnetisation was a linear function of the applied field. This behaviour is consistent with that of a paramagnet which freezes as a spin glass at 8 K. The hysteresis above the freezing temperature can be attributed to the presence of blocked spin clusters.

Analysis of the high temperature magnetic behaviour proved illuminating. Attempts to model the inverse susceptibility of $LaBaInMnO_6$ (Fig. 5a, inset) using the Curie–Weiss Law lead to a small, positive value of θ (Table 5). This is unrealistic, given that this composition contains only $Mn^{4+}:3d^3$ cations which will interact antiferromagnetically. Furthermore, the maximum molar susceptibility expected for this compound at 300 K can be estimated (6.25×10^{-3} cm^3 mol^{-1}) from the

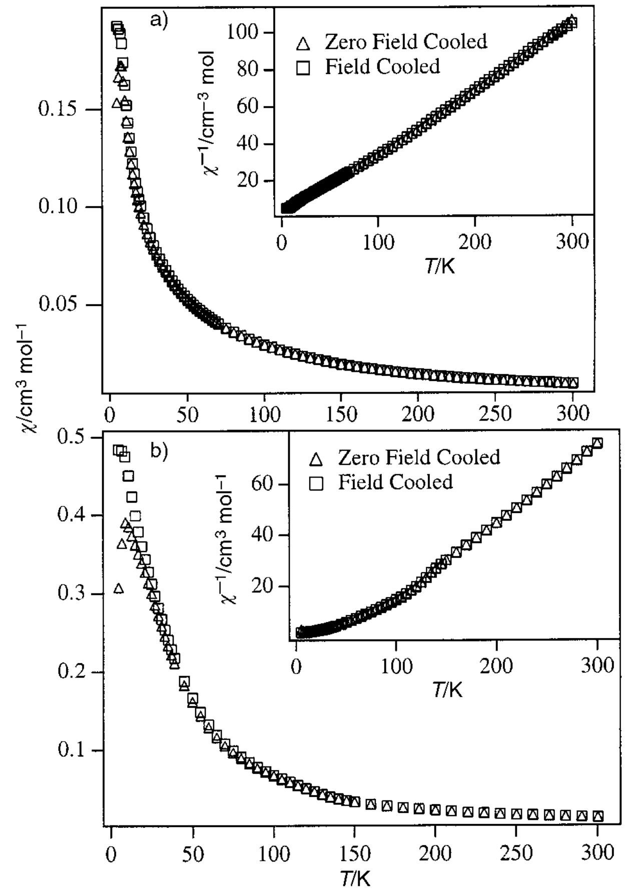

Fig. 5 Temperature dependence of the susceptibility of a) $LaBaInMnO_6$ and b) $La_{1.2}Ba_{0.8}InMnO_6$ in a measuring field of 100 Oe. The inset shows the inverse susceptibility data.

Table 5 Magnetic data for $La_{1+x}A_{1-x}InMnO_{6-\delta}$

	θ/K	C/cm^3 K mol^{-1}	μ_{eff}/μ_B per formula unit
$La_{1.0}Ba_{1.0}InMnO_{6-\delta}$	14.9(9)	2.70(1)	4.647(1)
$La_{1.2}Ba_{0.8}InMnO_{6-\delta}$	56.6(9)	3.24(2)	5.091(2)
$La_{1.2}Sr_{0.8}InMnO_{6-\delta}$	82(1)	2.62(3)	4.578(3)

spin-only moment of a d^3 cation (any orbital contribution to the moment will reduce the overall value) and it is less than the measured value. In order to rationalize these observations we assume that the composition of the sample is oxygen deficient, $LaBaInMnO_{6-\delta}$, and contains a small fraction of Mn^{3+} cations. If we take the value of the molar susceptibility of Mn^{3+} at 300 K from our study[6] of La_2GaMnO_6, we can deduce $\delta = 0.12$. We must emphasise that this value of δ is no more than an estimate, but our attempts to determine a better value by oxidising the sample under flowing oxygen gas were unsuccessful. Although our neutron study showed that there was no significant oxygen deficiency, test refinements demonstrated that our data analysis would be insensitive to such a low level ($\sim$2%) of anion vacancies. The presence of Mn^{3+} : d^4 not only accounts for the enhanced value of the susceptibility, but it also introduces the possibility of ferromagnetic σ superexchange between Mn^{3+} and Mn^{4+} cations, and therefore accounts for the positive value of θ. The values of χ_{300} and θ increase further when the concentration of Mn^{3+} is deliberately increased by doping with Ba, although the value of the Curie constant for $La_{1.2}Sr_{0.8}InMnO_6$ suggests that the concentration of oxide vacancies is lower in the Sr-containing material.

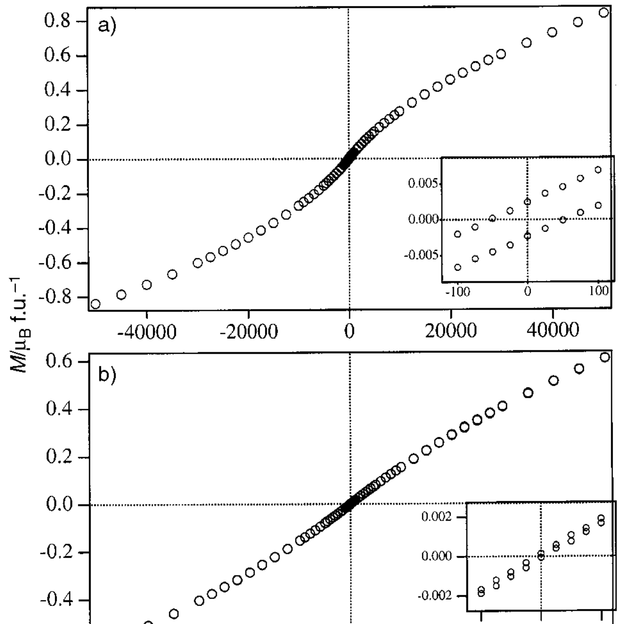

Fig. 6 Field dependence of the magnetisation of $LaBaInMnO_6$ at a) 5 K and b) 25 K.

The resistivity of $La_{1.2}Ba_{0.8}InMnO_6$ was activated ($E_a = 0.264(5)$ eV) throughout the measured temperature range ($164 \leqslant T/K \leqslant 300$); the resistance became immeasurably large at lower temperatures. A negative magnetoresistance $\Delta\rho/\rho_0 = 10.5\%$ was measured at 164 K in a field of 14 T. On the basis of this result we chose not to pursue the study of magnetotransport in this system.

Discussion

The X-ray diffraction data indicate that all the compounds synthesised have perovskite-related structures but that the nature of the tilting of the BO_6 octahedra is determined by the alkaline-earth cation present. The three-tilt system exhibited by $La_{1+x}Sr_xInMnO_6$ ($x = 0.2$) corresponds in Glazer's notation[12] to an $a^-b^+a^-$ tilting of the octahedra. This $GdFeO_3$ structure is frequently adopted by manganite perovskites. The two tilt system $a^-b^0a^-$ (Fig. 7) adopted by $La_{1+x}Ba_xInMnO_6$ is less common though a number of other examples have been reported, including $Nd_{0.5}Sr_{0.5}MnO_3$,[15] $Pr_{0.65}Ba_{0.35}MnO_3$[16] and $La_{0.7}Ba_{0.3}MnO_3$[17] amongst others.[18–20]

Both the X-ray and neutron diffraction data show that the B-site cations are disordered in all the samples synthesised. Previous studies[8] have shown that B-cations with significant differences in charge (greater than 2) and ionic radii (greater than 0.1 Å) have a tendency to order in the rocksalt arrangement, whilst it has been suggested that a layered structure, observed for La_2SnCuO_6,[21] can arise from a conflict between the preferred co-ordination geometry of the two B-site cations. Such layered arrangements of B cations are rare in perovskite related materials. As well as La_2SnCuO_6, alternative lanthanide cations have been incorporated into the Ln_2SnCuO_6 system (Ln = Pr, Nd, Sm) through the use of high pressure techniques[22] and La_2ZrCuO_6 has been synthesised using a similar protocol.[22] These systems both contain a spherical cation (Zr^{4+} or Sn^{4+}) and a Jahn–Teller active cation (Cu^{2+}). In the case of the manganese perovskites, it is shown here that substituting the B site with the spherical d^{10} cation, In^{3+}, results in a disordered arrangement on the B site. It should be noted that in $LaBaInMnO_6$ there would be no conflict in the preferred co-ordination geometry of the cations since Mn^{4+} has a d^3 electron configuration. In fact, it might be expected that the Mn^{3+}-rich compositions which we were unable to

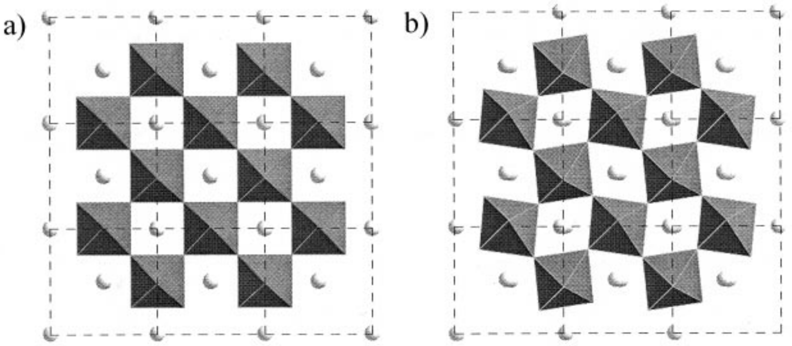

Fig. 7 View down [010] showing perovskites with a) a 2 tilt ($a^-b^0a^-$) system (*Imma*) and b) a 3 tilt ($a^-b^+a^-$) system (*Pnma*).

synthesize, for example La_2InMnO_6, would have been more likely to adopt a layered ordering pattern. However, it should be remembered that although La_2GaMnO_6 and Nd_2GaMnO_6 contain both a Jahn–Teller active cation (Mn^{3+}) and a d^{10} ion on the B site, and are thus analogous to La_2SnCuO_6, both species adopt a disordered arrangement of B cations.[9]

Spin-glass behaviour, attributed to the presence of competing magnetic interactions,[23] has previously been observed in perovskites with a 1 : 1 random distribution of d^3 cations (Ru^V) and another paramagnetic species on the B sites. Comparable examples involving Mn^{4+} are rare, although a recent study of $ALaMnFeO_6$ (A = Ba, Sr, Ca) showed that a disordered arrangement of Mn^{IV} and Fe^{III} results in the absence of magnetic ordering down to temperatures as low as 15 K (the limit of the experiment).[24] In a case where a non-magnetic ion (Zn^{2+}) was randomly substituted (50%) on to a B site containing Ru^{5+}, long range magnetic order was reported.[23,25] Fifty per cent dilution of the B site with diamagnetic cations would not be expected to destroy the magnetic backbone and create the degree of disorder usually required for spin glass formation, and the observation of long range order in $LaBaZnRuO_6$ was to be expected. (However, dilution of Fe^{3+} in a perovskite by the d^0 cations Ta^{5+} and Nb^{5+} has been shown to produce spin glass behaviour,[26] although dilution with d^{10} Sb^{5+} resulted in the retention of long-range magnetic ordering.[27]) In the light of these results, doping d^{10} : In^{3+} on to a sublattice containing only Mn^{4+} would not usually be expected to eliminate long-range magnetic ordering. The observation of spin glass behaviour in $LaBaInMnO_{6-\delta}$ is therefore best explained in terms of the competing interactions introduced by the presence ($\sim$25%) of Mn^{3+} on the nominal Mn^{4+} sublattice. The π superexchange interactions between these cations will be antiferromagnetic, whereas the σ interactions will be ferromagnetic. The interactions between pairs of neighbouring Mn^{3+} cations could be of either sign, depending on the nature of any local distortion of the coordination geometry which might be brought about by the degenerate electron configuration of the Jahn–Teller active cations. Spin glass behaviour has been observed previously in mixed valence $n = 2$ Ruddlesden–Popper manganites, for example $Sr_2YMn_2O_7$,[28] although in that case the octahedral sites were not diluted by a diamagnetic cation. In contrast, the diluted compound $La_{1.5}Sr_{0.5}MnRhO_6$, with Mn in a mean oxidation state of 3.5, is ferromagnetic below 105 K.[6,7] The results described above are consistent with the idea that the contrasting properties of the Rh- and In-containing compounds stem from the availability of empty e_g* orbitals on the diamagnetic dopant in the former, but not in the latter.

Conclusion

A number of new perovskites with a disordered 1 : 1 distribution of In^{3+} and $Mn^{3+/4+}$ on the B-sites have been synthesised and characterised. Diffraction data show that the two tilt system $a^-b^0a^-$ is adopted by $La_{1+x}Ba_xInMnO_{6-\delta}$ and the three tilt system $a^-b^+a^-$ by $La_{1+x}Sr_xInMnO_{6-\delta}$. The temperature dependence of the molar magnetisation shows these compounds to be spin glasses and low temperature neutron diffraction data have confirmed the lack of long range magnetic order in $LaBaInMnO_6$.

Acknowledgements

We are grateful to Dr. T. Hansen at the ILL, Grenoble for experimental assistance with the neutron diffraction experiments and to the UK Engineering and Physical Science Research Council for funding.

References

1 B. Raveau, C. Martin and A. Maignan, *J. Alloys Compd.*, 1998, **277**, 461.
2 A. Maignan, F. Damay, A. Barnabé, C. Martin, M. Hervieu and B. Raveau, *Philos. Trans. R. Soc. London A*, 1998, **356**, 1635.
3 F. Damay, C. Martin, A. Maignan and B. Raveau, *J. Magn. Magn. Mater.*, 1998, **183**, 143.
4 B. Raveau, Y. M. Zhao, C. Martin, M. Hervieu and A. Maignan, *J. Solid State Chem.*, 2000, **149**, 203.
5 P. D. Battle, J. C. Burley, E. J. Cussen, G. C. Hardy, M. A. Hayward, L. D. Noailles and M. J. Rosseinsky, *Chem. Commun.*, 1999, 1977.
6 B. Bakowski, P. D. Battle, E. J. Cussen, L. D. Noailles, M. J. Rosseinsky, A. I. Coldea and J. Singleton, *Chem. Commun.*, 1999, 2209.
7 A. I. Coldea, I. M. Marshall, S. J. Blundell, J. Singleton, L. D. Noailles, P. D. Battle and M. J. Rosseinsky, *Phys. Rev. B*, 2000, **62**, 6077.
8 M. T. Anderson, K. B. Greenwood, G. A. Taylor and K. R. Poeppelmeier, *Prog. Solid State Chem.*, 1993, **22**, 197.
9 E. J. Cussen, M. J. Rosseinsky, P. D. Battle, J. C. Burley, L. E. Spring, J. F. Vente, S. J. Blundell, A. I. Coldea and J. Singleton, *J. Am. Chem. Soc.*, 2001, **123**, 1111.
10 H. M. Rietveld, *J. Appl. Crystallogr.*, 1969, **2**, 65.
11 A. C. Larson and R. B.von Dreele, 1990, Report LAUR 86-748.
12 A. M. Glazer, *Acta Crystallogr., Sect. B*, 1972, **28**, 3384.
13 V. F. Sears, *Neutron News*, 1992, **3**, 26.
14 R. D. Shannon, *Acta Crystallogr., Sect. A*, 1976, **32**, 751.
15 V. Caignaert, F. Millange, M. Hervieu, E. Suard and B. Raveau, *Solid State Commun.*, 1996, **99**, 173.
16 Z. Jirak, E. Pollert, A. F. Anderson, J.-C. Grenier and P. Hagenmuller, *Eur. J. Solid State Inorg. Chem.*, 1990, **27**, 421.
17 P. G. Radaelli, M. Marezio, H. Y. Hwang and S.-W. Cheong, *J. Solid State Chem.*, 1996, **122**, 444.
18 P. M. Woodward, T. Vogt, D. E. Cox, A. Arulraj, C. N. R. Rao, P. Karen and A. K. Cheetham, *Chem. Mater.*, 1998, **10**, 3652.
19 A. Sundaresan, V. Caignaert, A. Maignan and B. Raveau, *Phys. Rev. B*, 1999, **60**, 533.
20 Z. Jirak, F. Damay, M. Hervieu, C. Martin, B. Raveau, G. André and F. Bourée, *Phys. Rev. B*, 2000, **61**, 1181.

21 M. T. Anderson and K. R. Poeppelmeier, *Chem. Mater.*, 1991, **3**, 476.

22 M. Azuma, S. Kaimori and M. Takano, *Chem. Mater.*, 1998, **10**, 3124.

23 P. D. Battle, T. C. Gibb, C. W. Jones and F. Studer, *J. Solid State Chem.*, 1989, **78**, 281.

24 K. Ramesha, V. Thangadurai, D. Sutar, S. V. Subramanyam, G. N. Subbanna and J. Gopalakrishnan, *Mater. Res. Bull.*, 2000, **35**, 559.

25 K. Hong, Y. Choi, Y. Kwon, D. Jung, J. Lee, H. Shim and C. Lee, *J. Solid State Chem.*, 2000, **150**, 383.

26 P. D. Battle, T. C. Gibb, A. J. Herod, S. J. Kim and P. H. Munns, *J. Mater. Chem.*, 1995, **5**, 865.

27 E. J. Cussen, J. F. Vente, P. D. Battle and T. C. Gibb, *J. Mater. Chem.*, 1997, **7**, 459.

28 P. D. Battle, J. E. Millburn, M. J. Rosseinsky, L. E. Spring, J. F. Vente and P. G. Radaelli, *Chem. Mater.*, 1997, **9**, 3136.